Accurate Modeling of Quality Factor Behavior of Complex Silicon MEMS Resonators

Shirin Ghaffari, Eldwin Jiaqiang Ng, Chae Hyuck Ahn, Yushi Yang, Shasha Wang, Vu A. Hong, and Thomas W. Kenny

Abstract— **The quality factor of a resonator represents the decay of vibrational energy over time, and is directly related to the frequency response and other key parameters that determine performance of inertial sensors and oscillators. Accurate prediction of the quality factor is essential for designing high-performance microelectromechanical (MEMS) devices. Several energy dissipation mechanisms contribute to the quality factor. Due to computational complexity, highly simplified models for the dominant dissipation mechanism, such as Zener's model for thermoelastic dissipation (TED), are often employed. However, the intuition provided by these models is inadequate to predict the quality factor of more complex designs and can be highly misleading. In this paper, we construct complete, quantitative, and predictive models with finite-element methods for the intrinsic energy dissipation mechanisms in MEMS resonators using full anisotropic representation of crystalline silicon and the temperature dependence of all parameters. We find that TED is often a more significant source of damping than has been assumed, because of the previously neglected role of crystalline anisotropy and small geometric features, such as etch release holes—all of which can now be included in practical models. We show that these models, along with simpler scaling models for extrinsic dissipation mechanisms, explain measurements of quality factor in diverse sets of MEMS resonators with unprecedented accuracy. [2014-0106]**

Index Terms— **Capacitive sensors, damping, energy dissipation, frequency response, frequency-domain analysis, geometry, internal friction, microelectromechanical systems (MEMS), microelectromechanical devices, micromechanical resonators, physics, Q-factor, quality factor, resonance, thermoelastic dissipation, thermal-mechanical coupling.**

I. Introduction

THE PERFORMANCE of a Microelectromechanical (MEMS) resonator depends significantly on the rate at which the vibrational energy of the resonator is dissipated. The quality factor Q is a measure of the time rate of decay of the resonator vibration energy and is defined as the ratio of the maximum strain energy to the dissipated energy per cycle. High values of Q correspond to a longer decay time and vice versa. The ability to accurately model the Q of MEMS resonators is crucial for designing devices with predictable or optimized Q.

TABLE I
TYPICAL MEASURED FREQUENCY f AND QUALITY FACTOR Q OF RESONATORS STUDIED FOR THIS WORK AT ROOM TEMPERATURE

Device	*DETF*	*DRG*	*Dual ring resonator*
f (MHz)	1.3	0.247	19.7
Q	10,000	100,000	150,000

The quality factor of MEMS resonators have been extensively studied [1]–[33]. For more simple designs, such as beams, Q has been modeled fairly accurately [5], [6], however the body of modeling work that quantitatively predicts or explains measurement results for more complex designs is very limited. This paper presents a detailed modeling approach and quantitative results for Q of a diverse set of MEMS resonators that compare with measurements with unprecedented accuracy.

We study three distinct types of resonators: a double ended tuning fork (DETF), a disk resonator (DRG), and a dual ring resonator. Table I shows typical frequency f and quality factor Q of this set of devices and the resonator designs are illustrated in Figure 1. The resonators span an order of magnitude in f and Q. Among those, the DRG has the lowest f, and a corresponding Q comparable to that of the dual ring resonator. The DETF operates at an intermediate f and has the lowest Q among others. The quality factor of various resonators depends on a combination of several dissipation mechanisms, as will be discussed in this paper. It is interesting from the design standpoint that these variations in Q are readily achieved with comparable feature size, and in the same material fabricated in a single process.

All of the experimental results presented in this paper are from devices fabricated in the epitaxial polysilicon encapsulation process. The *epi-seal* encapsulation process was proposed by researchers at the Robert Bosch Research and Technology Center in Palo Alto and then demonstrated in a close collaboration with Stanford University. This collaboration is continuing to develop improvements and extensions to this process for many applications, while the baseline process has been brought into volume production at Tower-Jazz by SiTime. Among the benefits of this process are hermetic encapsulation at

Manuscript received March 31, 2014; revised August 8, 2014; accepted August 13, 2014. Date of publication December 22, 2014; date of current version March 31, 2015. This work was supported in part by the Defense Advanced Research Projects Agency through the Precision Navigation and Timing Program under Grant N66001-12-1-4260 and Grant N6601-12-C-4178, and in part by the National Science Foundation through the National Nanotechnology Infrastructure Network under Grant ECS-9731293. Subject Editor G. Piazza.

S. Ghaffari and S. Wang are with Apple Inc., Cupertino, CA 95014 USA (e-mail: ghaffari@stanford.edu; wangss@stanford.edu).

E. J. Ng, C. H. Ahn, Y. Yang, V. A. Hong, and T. W. Kenny are with Stanford University, Stanford, CA 94305 USA (e-mail: eldwin@stanford.edu; ahn1229@stanford.edu; ysyang88@stanford.edu; tkenny@stanford.edu).

Color versions of one or more of the figures in this paper are available online at http://ieeexplore.ieee.org.

Digital Object Identifier 10.1109/JMEMS.2014.2374451

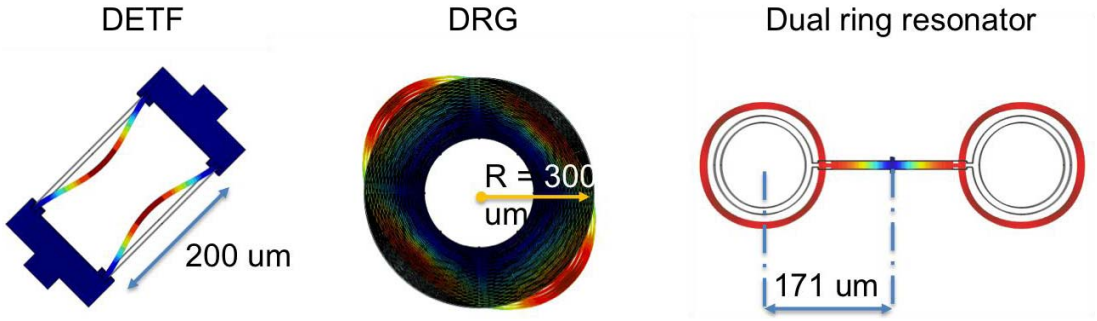

Fig. 1. FEM simulation of the deformation mode shape of the three resonators colored with relative total displacement. Mode shapes correspond to first bending harmonic of the DETF, wine glass mode of the DRG and contour extension (breathe) mode of the dual ring resonator.

low pressure, sidewall smoothing by hydrogen annealing [34] high yield and low-cost manufacturing in a foundry compatible process. Many previous academic publications relied on processes where the resonators and the anchors are defined in separate steps, and misalignments lead to enhancement of loss through the anchors, contributing to a widely-held perception that anchor damping is a fundamental limit to resonators such as the devices in this study. An important feature of our fabrication process is that all geometric features, including resonator, electrodes, gaps, and anchors, are defined in a single, early lithographic and etching step. Because of this capability, we are able to design resonators with anchors precisely-located at the nodal points of the vibrational modes being studied, which greatly reduces anchor damping in all the resonators for this study.

Two categories of energy dissipation are present in models for the Q: extrinsic losses, such as anchor damping and pressure damping, and intrinsic losses such as thermoelastic dissipation (TED) and Akhiezer damping (AKE). Because independent contributions of the dissipation mechanisms to the total energy dissipation are considered and Q is proportional to the inverse of total energy dissipated, the Q of the resonator can be represented as a reciprocal sum of independent dissipative contributions,

$$\frac{1}{Q_{measured}} = \sum \frac{1}{Q_{pressure}} + \frac{1}{Q_{anchor}} + \frac{1}{Q_{TED}} + \frac{1}{Q_{AKE}}. \tag{1.1}$$

II. Methods

A comprehensive approach is used to model the Q and f behavior of the resonators. We obtain the Q contribution from TED, computationally from high fidelity finite element method (FEM) simulations [5] and the Q contribution of AKE from an a-priori analytical model [10]. The contribution from pressure damping is evaluated from independent measurements of the pressure in the packages built with these devices, and a scaling model based on the temperature dependence of pressure damping. Sometimes, a residual contribution from anchor damping is included. This contribution is evaluated by fitting a temperature-independent contribution to the experimental data after all other known mechanisms have been applied. In these devices, anchor damping is not expected to dominate, because the observed, relatively strong temperature dependence of Q for these devices is inconsistent with the expected, relatively weak temperature dependence of anchor damping. Further, as will be shown, the measurements of Q over temperature for these devices are fully accounted for without substantial contributions from anchor damping. No conditions are imposed on modeling to compare with measurements, and no materials parameters are adjusted to improve the fits of the models to the data.

The resonant frequency of the modeled devices is obtained from FEM simulation of the free dynamic response of the resonator. The mechanical frequency is the real part of complex eigenvalue of the coupled thermoelastic equations. Since TED, as we shall see, is significant in these resonators, it is necessary to obtain the frequency from fully coupled simulations. Through this approach, the coupling effect of thermal expansion, although small, is retained in the model and this calculation comes at no extra computational cost beyond the calculation of TED.

Pressure damping is due to dissipative forces acting on the surface the resonator. There is always a finite contribution of pressure damping depending on the vacuum level of the resonator cavity, and the detailed shapes of the moving surfaces. In the general case of a resonator, the pressure-contribution to Q has a well known scaling with pressure P of the gas in the cavity and the temperature T [24],

$$Q_{pressure} \sim \frac{\omega\sqrt{k_B T}}{P}. \tag{2.1}$$

where $\omega = 2\pi f$ and k_B is Boltzmann constant. All of our devices are hermetically sealed with epi-seal process [35] and annealed at high temperature ~1000 °C. The gas in the cavities is low pressure (~20 mTorr or less) and is composed almost entirely of H_2. The gas may be assumed to behave as an ideal gas with a fixed number density, so pressure is proportional to temperature $P \sim T$. The quality factor, therefore, has a unique relation with temperature, $Q_{pressure} \sim T^{-1/2}$, and the signature of this contribution can be recognized from experimental measurements. Even without detailed computations of the amplitude of pressure damping, we can use this 'signature' to identify its presence and determine its magnitude, by comparing models and measurements over temperature. Therefore, we use this temperature-dependent scaling of the pressure contribution to Q in order to identify and determine the contribution of pressure damping in the measurements.

The cyclic forces and moments that resonator oscillation exerts on its anchors can excite shear and normal stress waves that propagate into the substrate; part of energy of these stress waves is absorbed by the anchors and the substrate and is dissipated. This phenomenon is referred to as anchor damping [36]–[42]. In the simple case of the first harmonic bending of a uniform rectangular thin beam with length L and width w, for example, it may be shown that Q is proportional to the beam aspect ratio $(L/w)^3$ to within a constant $Q_{anchor} \sim C(L/w)^3$ [37]. The prefactor is a function of the mode shape but it is independent of the elastic modulus, and the remaining scaling depends entirely on dimensions. Therefore, anchor damping is expected to be approximately constant over temperature. We use this temperature-independent characteristic of anchor damping to help identify and determine the contribution of anchor damping in the measurements.

During the vibration of the crystal, strain disturbs the local thermal equilibrium and this equilibrium is eventually restored by inelastic phonon scattering processes. If this phonon scattering process happens at a timescale faster than the period of the oscillation, it leads to dissipation which is referred to as Akhiezer effect (AKE) [43]. This thermalization timescale τ for silicon is of order 0.1 nS or faster, so we can expect AKE dissipation to be significant for resonators with frequencies below 10 GHz. To calculate the Q contribution of AKE, we use the predetermined relation based on frequency f and material properties of single crystal silicon [10], [44],

$$Q_{AKE} = \frac{\rho c^4}{2\pi \gamma_{avg}^2 kTf} \tag{2.2}$$

where ρ, c, and k are, respectively, density, the average speed of sound and the thermal conductivity. γ_{avg} is the average Grüniesen's parameter and T is the temperature. Among these factors, Grüniesen's parameter is most difficult to estimate, as it depends on the details of the phonon spectrum, the polarization of the phonons and many other factors that cannot be represented as a single materials-dependent parameter. The uncertainty in the amplitude of this dissipation mechanism may be as large as an order of magnitude, and this uncertainty is reflected in our models and used in comparisons with our measurements.

III. Analysis of Thermoelastic Dissipation (TED)

The general governing equations for thermoelastic dissipation are the coupled equations of motion and heat conduction [5], [45],

$$-\rho\omega_j^2 u = \nabla \cdot \sigma \tag{3.1}$$

$$\rho c_p i\omega_j T - \nabla \cdot (k\nabla T) = -i\omega_j T_0 \alpha \cdot \sigma \tag{3.2}$$

where ω_j is the complex frequency of the jth vibration mode with the displacement field $u = (u, v, w)$, and T_0 denotes the ambient temperature. α and k are respectively the thermal expansion coefficient and thermal conductivity. The stress $\boldsymbol{\sigma}$ is calculated from Hooke's law relation $\boldsymbol{\sigma = C(\epsilon - \alpha T)}$ where $\boldsymbol{\epsilon}$ is the strain tensor and C is the anisotropic elastic tensor. This representation takes into account elastic anisotropy.

The coupling terms on the right hand sides of Eq. (3.1) and Eq. (3.2) are often very small relative to the other terms and can be neglected in many resonator analyses, especially those that are known to be dominated by pressure damping, anchor damping or other mechanisms. However, the effects that arise from these coupling terms can be important in resonators that are protected from these other damping mechanisms. Using modern simulation tools, it is practical to consider the fully-coupled case, and solvers that utilize the fully-coupled model are in wide use [30]–[32], [46]. Because of this practicality, we encourage the use of these models even in cases where the researchers believe that other mechanisms are dominant. We find that TED models that include the complete crystal anisotropy and all geometric details may show that TED is playing a more significant role than expected.

The well-known Zener's approximation [1], [2] for TED leads to a simple analytical expression for Q, which has provided an intuitive guide to MEMS designers. The expression for Q has a prefactor that is a function of material properties. The material prefactor has been a basis for comparing and selecting candidate materials for MEMS Resonators [56], [57]. For example, materials with low coefficient of thermal expansion α could have reduced TED. The problem with some low TCE material such as fused silica is that it suffers from other loss terms, and may never reach the TED limit [57]. In general, the material prefactor from the simplified zener model is useful to consider, but given the availability of efficient computational tools, we now strongly encourage designers to carry out detailed modeling of their particular designs, using a complete set of materials properties. This approach can allow better materials selection as well as geometric design optimization to be completed prior to initiating much more expensive fabrication process development and empirical device studies.

The simple form of Zener's equation is convenient but it is inadequate for predicting Q of more complex designs than a homogeneous thin beam. For example, Candler et al. demonstrated that Zener's formula substantially underestimates the measured Q of tuning forks with slots that were added to suppress the heat transfer [6].

A. Computational Model

Here, we are interested in the free vibration of the resonator, and therefore in the computational model resonator boundaries are assumed free except at anchors where they are fixed. In the absence of external heating, the resonator boundaries also may be assumed to be thermally insulated. Because the damped eigenfrequencies are the solutions of the unforced thermoelastic equations, surface traction is also zero. With these boundary conditions, the set of linear equations (3.1)-(3.2) reduces to a general eigenvalue problem [58].

The complete eigenvalue problem of (3.1)-(3.2) can be solved with a finite element (FE) solution method using commercial FEM software of choice, and is equally applicable to arbitrary structures. The results presented in this paper are from the implementation of the problem in COMSOL Multiphysics v4.3a [46].

To solve the TED problem, two physical domains are invoked; *solid mechanics* and *heat transfer* and we define the proper coupling terms to fully couple the two. The equations of motion (3.1) correspond to a *linear elastic solid* with *thermal expansion*.

We may conveniently add the harmonic terms of Eq. (3.2) into a heat source term q for the heat conduction equation.

$$q = -\omega_i(\rho c_p T + T_0 \alpha \cdot \sigma) \tag{3.3}$$

The second term in parentheses can be expanded as,

$$\alpha \cdot \sigma = [\alpha_{11}\ \alpha_{22}\ \alpha_{33}\ 2\alpha_{23}\ 2\alpha_{13}\ 2\alpha_{12}][\sigma_x\ \sigma_y\ \sigma_z\ \sigma_{yz}\ \sigma_{xz}\ \sigma_{xy}]^T \tag{3.4}$$

This implementation of the heat source is general and can be applied to an arbitrary anisotropic solid. For single crystal silicon (SCS), α is isotropic and the vector is simplified to a scalar multiplier. Due to anisotropic elasticity however, the full stress vector must be retained. The heat flux at the exterior boundaries is set to zero.

To obtain a fully coupled system, the strain induced temperature calculated in Eq. (3.2) is defined as input temperature for the thermal expansion term in Eq. (3.1).

In harmonic form, the heat conduction equation is time independent and to perform an *eigenfrequency study*, the heat transfer model must be appropriately solved in *stationary* form. Finally the coupled eigenvalue problem of (3.1)-(3.4) is solved for desired number of frequencies.

The Q of the resonator is defined as the ratio of the maximum strain energy to the dissipated energy per cycle. In the limit of small decay rates, we may obtain Q from the complex eigenvalue ω solution of the coupled TED equations for a general anisotropic solid:

$$Q = \frac{1}{2}\frac{\Re(\omega)}{\Im(\omega)} \tag{3.4}$$

A later version of COMSOL has built in an implementation of (3.1)-(3.4) in a *thermoelasticity* module. The methods described in this section are generally applicable and explain the steps to model TED accurately if properly used within any FEM software. All of these implementations produce the same results, within numerical solver variations and roundoff error effects.

B. Anisotropy of Material Properties

The appropriate anisotropic representation for the resonator structure is the one for which the coordinate system aligns with the stress axes of interest. The stress axes are the device material axes for any orientation in the reference frame of the wafer. The anisotropy can be aligned with the structure orientation by rotating the design plane by the angular deviation of the structure from the (100) plane. However, if the structure has planar symmetries, it is invariant to that rotation. In general, the anisotropy axes are obtained from rotation of the elasticity matrix.

The rotated elasticity matrix in the nominal [110] frame of wafer is found by a 45° in plane rotation of the standard (100) elasticity or calculated from SCS orthotropic relations [48] for Young's modulus E, shear modulus G, and Poisson's ratio v in the frame of the wafer as given in Table II.

TABLE II
VALUES OF THE YOUNG'S MODULUS E, SHEAR MODULUS G, AND POISSON'S RATIO IN THE FRAME OF THE STANDARD (100) WAFER [48]

$\boldsymbol{E}$	*value (GPa)*	$\boldsymbol{G}$	*value (GPa)*	$\boldsymbol{v}$	*value*
E_x	169	G_{xz}	76.9	v_{xz}	0.28
E_y	169	G_{yz}	76.9	v_{yz}	0.36
E_z	130	G_{xy}	50.9	v_{xy}	0.064

TABLE III
COMPARISON OF QTED FROM ANISOTROPIC AND ISOTROPIC TED SIMULATIONS WITH QUALITY FACTOR MEASUREMENTS FOR A DOUBLE ENDED TUNING FORK (DETF), A DISK RESONATOR (DRG) AND A DUAL RING RESONATOR. THE RESONATOR DESIGNS ARE SHOWN IN FIGURE 1

	DETF	*DRG*	*Dual ring resonator*
Measured Q	9,400	100,000	155,000
Anisotropic Q_{TED}	11,000	131,000	153,000
Isotropic Q_{TED}	10,900	214,000	2,000,000

Anisotropy will have a significant effect on the Q of TED where strain gradients due to anisotropy dominate the strain gradients in the mode shape. The effect is largest in resonators that operate with uniform strains such as the extensional (breathe) mode ring resonator, because the anisotropy becomes the dominant source of strains in these devices. In Table III we compare the isotropic and anisotropic simulated value of the Q of TED for the various resonator geometries and mode shapes to the measured Q. For the three simulations, the isotropic value of the Young's modulus was properly chosen that of the wafer ⟨110⟩ axis E = 169 GPa which is the X axis of the resonators layout.

It is evident that anisotropy must be incorporated in order to accurately predict the Q of the dual ring resonator where the mode shape has small strain gradient. For the disk resonator, the isotropic simulation ignores the different stiffnesses of the two axes of the mode. The contribution of anisotropy to TED is at least 60% in this case. Strain in the tuning fork resonator however is expected to be dominantly set by the stiffness of the bending axis. Since the complete anisotropic elasticity data is readily available for Silicon [48], and easily utilized in these computational models, we recommend that the full anisoptropic model be used in any simulations.

C. Temperature Dependence

The temperature dependence of the resonator frequency predominantly results from the temperature dependence of the elastic moduli. Table IV shows the values of first and second temperature coefficients of the elastic constants for low-doped p-type silicon, which is commonly used for MEMS devices, and is the material used for the devices studied in this paper.

TABLE IV
ELASTIC CONSTANTS AND THEIR FIRST AND SECOND TEMPERATURE COEFFICIENTS FOR LOW DOPED P-TYPE SILICON FROM [66]

c	value (GPa)	$TCc^{(1)}$	value ($ppm.C^{-1}$)	$TCc^{(2)}$	value ($ppb.C^{-2}$)
c_{11}	165.7	$TCc_{11}{}^{(1)}$	-73.25	$TCc_{11}{}^{(2)}$	-49.26
c_{12}	63.9	$TCc_{12}{}^{(1)}$	-60.14	$TCc_{12}{}^{(2)}$	-51.28
c_{44}	79.5	$TCc_{44}{}^{(1)}$	-91.59	$TCc_{44}{}^{(2)}$	-32.70

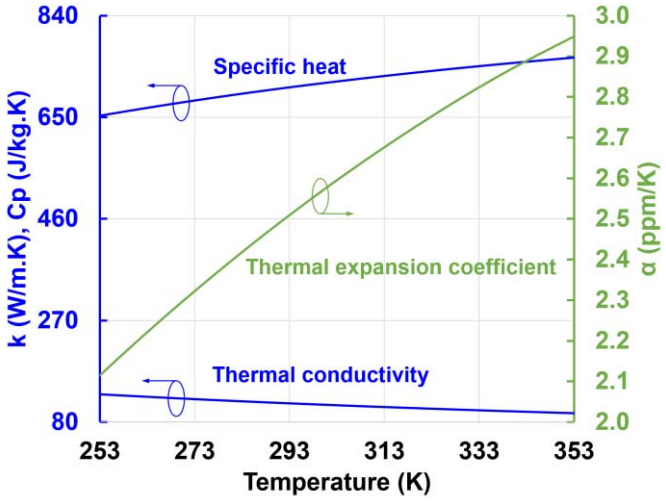

Fig. 2. Temperature dependence of specific heat [67], thermal expansion coefficient [68] and thermal conductivity [69] of single crystal silicon over the range T = 253 - 353 K.

The elastic constants are given in the [100] crystal frame. These values are applicable to low to moderate level doping of p-type devices, however the values can reasonably vary by at least 10% across the wafer. Elasticity as a function of doping type and level is explained as an electronic effect due to change in the electronic band energies [60], [61]. Recent results from measurement of temperature dependence of frequency for various doping levels and orientation show a strong doping effect [64], results clearly indicate mode sensitivity to doping levels which is due to the change of elastic constants. Some researchers have shown that resonators made with heavily doped silicon can exhibit total suppression of the first temperature coefficient, leading to MEMS resonators that are comparable in temperature dependence of frequency to AT-cut quartz crystals [60]–[64]. We have recently extracted a full set of temperature-dependent elastic constants for highly-doped silicon, which can be used with other results in this paper to design and predict dissipation in highly-doped silicon resonators [65].

To accurately predict the temperature dependence of Q, the temperature dependence of all the relevant material properties should also be carefully accounted for in the models for all dissipation mechanisms. Figure 2 shows the temperature dependence of the specific heat, the thermal expansion coefficient and the thermal conductivity of single crystal silicon [66]–[69] over the range T = 253 - 353 K. The models presented in this work are based on these data. For example, at room temperature, we use the following parameters, taken from these prior publications.

TABLE V
ROOM TEMPERATURE VALUES AND UNCERTAINTY IN MATERIAL PROPERTIES OF SINGLE CRYSTAL SILICON FROM [66]–[69]

TCc	α (ppm /°C)	k (W/kg.K)	C_p (J/kg.K)
Table IV	2.55	113.5	711.7
±10%	±5%	±15%	±5%

The exact value of the material properties over temperature depends on the experimental sample and the testing conditions, and we rely only on the published data presently available in this study. For each reference relied upon, some uncertainty in the reported values is accounted for. The uncertainties in the material properties for bulk silicon are summarized in Table V.

The fully coupled TED model, and the model for AKE depend on the temperature by way of temperature dependence of all material properties. The temperature dependence of the Q is not unique and also depends on the complex resonant frequency and the mode shape. Even within Zener's highly-approximated formulation, it is clear that there are no broadly accurate statements which can be made about materials choice or design.

In the next sections of this manuscript, we provide simulation results for TED using the fully-coupled formulation and the full anisotropy and temperature dependence of all relevant mechanical properties of silicon as discussed here. Our estimation of AKE is based on the same materials parameters. Using these models in combination with scaling models for pressure and anchor damping, we are able to fully account for the measured quality factor of a suite of distinct resonators, even including different orientations, and also including the measured temperature dependence of the Q. This approach does not utilize any adjustable parameters or simplifying assumptions about the resonator design. We show simulation results of a diverse set of resonators where the overall predicted quality factor and its temperature dependence match the experimental measurements closely. To our best knowledge these results are the most accurate predictions of Q over temperature for a diverse set of MEMS resonators.

IV. RESULTS

A. Double Ended Tuning Fork (DETF)

Our group has used the DETF as a reference device for many years [6], [24], [51] The DETF features familiar and consistent characteristics and is easily operated. The DETF has been known to be limited by TED, even in models which do not incorporate the crystalline anisotropy [17]. Our results incorporate the full anisotropy, as well as the temperature dependence of all relevant parameters, and provide a more accurate representation of the total set of contributions to the Q.

Figure 3 compares the measured and simulated frequency of the DETF over temperature for a resonator with beams aligned

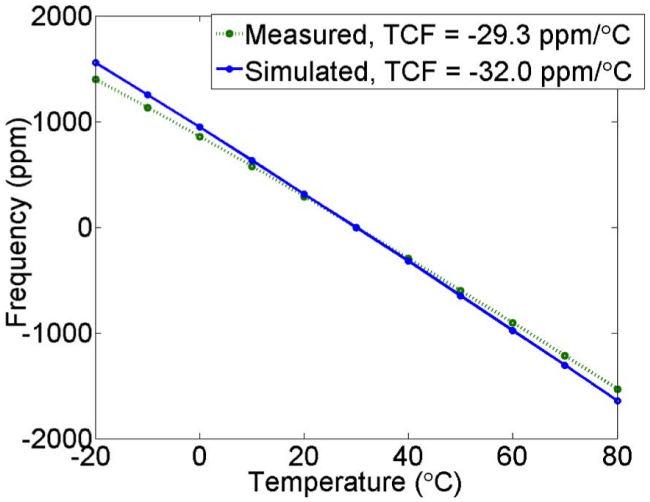

Fig. 3. Measured and simulated frequency of a DETF in ⟨110⟩ crystal direction over temperature. Error bars are too small to show.

TABLE VI
COMPARISON OF QUALITY FACTOR AT ROOM TEMPERATURE FOR A DETF IN [110] DIRECTION. QMEAS FROM MEASUREMENT, QTED FROM FULLY COUPLED SIMULATION AND QAKE FROM AKHIEZER MODEL OF (2.2)

Q_{meas}	Q_{TED}	Q_{AKE}
9,400	11,000	19,000,000

with the ⟨110⟩ crystal direction of a standard (100) wafer. The value of measured and simulated temperature coefficient of frequency TCF are within 10%, which is within the uncertainty of the values of the elastic constants that can arise from uncertainty in doping level for these devices. Overall, the TCF closely matches the analytical estimate from the temperature dependence of the elastic constants ~ -30 ppm/°C. The simulated frequency at each temperature is the real part of the complex eigenfrequency of a fully coupled TED simulation. The measurements are taken inside a temperature-stabilized oven at each point and each frequency data point is obtained from the average of 15 measurements. We have performed many similar measurements on many similar devices, and the TCF reported here is consistent with all past measurements on these devices, when oriented and doped in this manner.

The measured and modeled values of Q at room temperature are compared in Table VI. From this result, it is clear that the TED contribution cannot fully account for the total Q, and that the Akheizer term is far too weak to account for the difference. As a result, we consider the possibility that anchor damping and pressure damping may account for the difference. On the basis of this single measurement, it is impossible to identify anchor damping or pressure damping as the most important added contribution, so we carry out a set of experiments over temperature, and using different orientations in order to identify and isolate these extrinsic contributions from the directly-predicted intrinsic contributions.

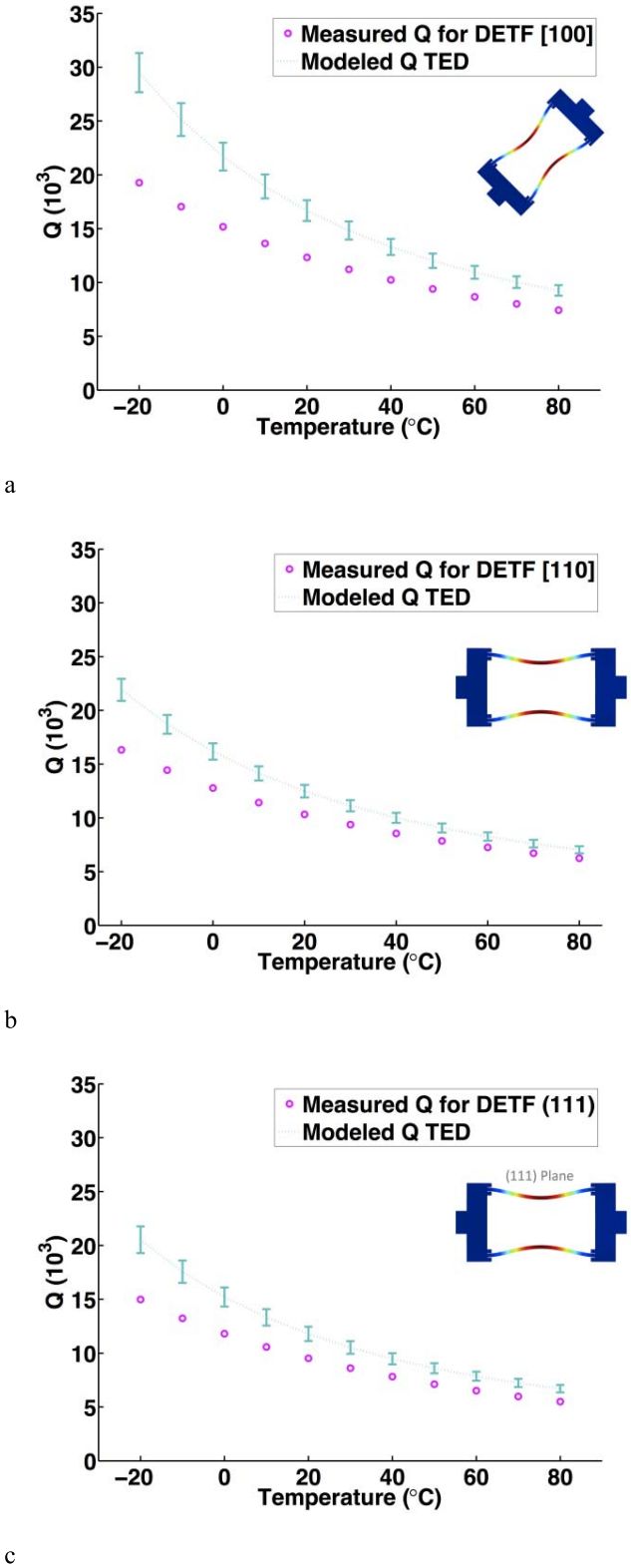

Fig. 4. Measured and simulated Q of DETFs in various crystal orientations. The beams align with the directions a) ⟨100⟩ b) ⟨110⟩, and c) ⟨110⟩ in the (111) plane. The dashed line goes through the values of the fully coupled TED simulations with typical material properties of SCS and the error bars correspond to simulated Q with uncertainty in the material properties as in Table V. Error bars on measured data points are too small to show.

Figure 4 shows measured Q and simulations of TED over a range of temperature for three different orientations of the DETF. In these experiments, Q decreases with the

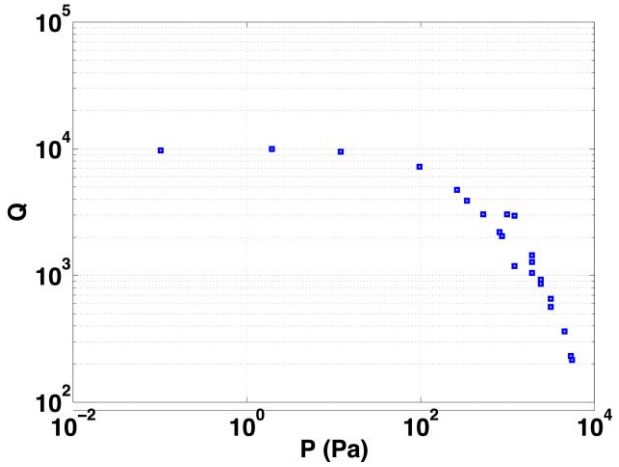

Fig. 5. Measured pressure dependence of quality factor of a representative DETF reproduced from [70].

stiffness of the bending axis as we vary orientation away from the ⟨110⟩ crystal direction. The resonators in the (111) wafer and oriented in the ⟨110⟩ direction correspond to the same crystal orientation and therefore comparable values of Q are expected. The error bars shown together with the simulation results correspond to the overall uncertainty in all material properties as given in Table V, whereas the error bars shown with the experimental results represent the standard deviation of the measured values of Q.

It can be seen that the predicted Q from TED is more sensitive to the values of the materials properties as well as the uncertainty in the values of those material properties at the lowest temperatures.

In a previous experiment [70], a focused ion beam tool was used to create a small opening in the encapsulation of a representative sealed DETF, and independently measured the Q as a function of pressure in a vacuum system as shown in Figure 5. From this independent experiment, we find that the Q of the sealed resonator matches the Q of the vented resonator at a chamber pressure of ∼30 Pa, and that the Q of a resonator at very low pressure rises to more than 10,000, in agreement with the TED model for this device.

In order to account for the complete effect of pressure damping, we compare the measured Q with a model based on the TED and the pressure contributions to the total as $Q_{model}^{-1} = Q_{TED}^{-1} + Q_{pressure}^{-1}$ over temperature, based on the temperature scaling of pressure as described as well as the complete model for the temperature dependence of TED. The pressure of the cavity from the fitted model is estimated to be between 20-40 Pa. We obtain the mean Q contribution of pressure damping with a single 30 Pa pressure in all orientations that matches the encapsulated pressure extracted from the independent measurements of $Q(P)$. With the addition of this contribution from pressure damping, the modeled Q accurately and quantitatively matches the measurements of Q in all three orientations, and over temperature as shown in Figure 6. We conclude that Q of DETFs is TED limited and is fully explained by a combination of TED and pressure damping.

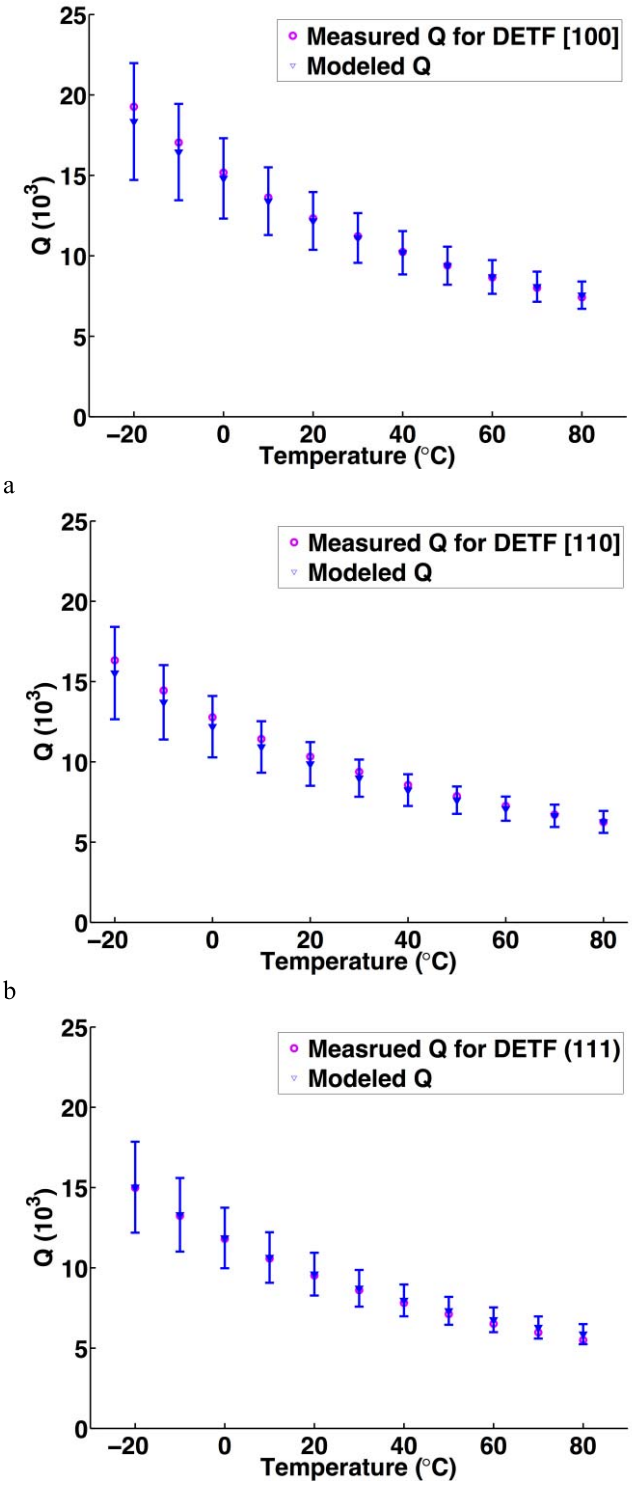

Fig. 6. Measured and overall modeled Q of DETFs in various crystal orientations: (a) ⟨100⟩ (b) ⟨110⟩, and (c) ⟨110⟩ in the (111) plane. Modeled Q values represent $Q_{model}^{-1} = Q_{TED}^{-1} + Q_{pressure}^{-1}$. The model for $Q_{pressure}$ uses a single 30 Pa pressure for the three orientations and the corresponding uncertainty in the pressure measurement.

In the case of these DETFs, we are able to account for the temperature dependence of the Q by incorporating a model based on TED with the temperature-dependent and

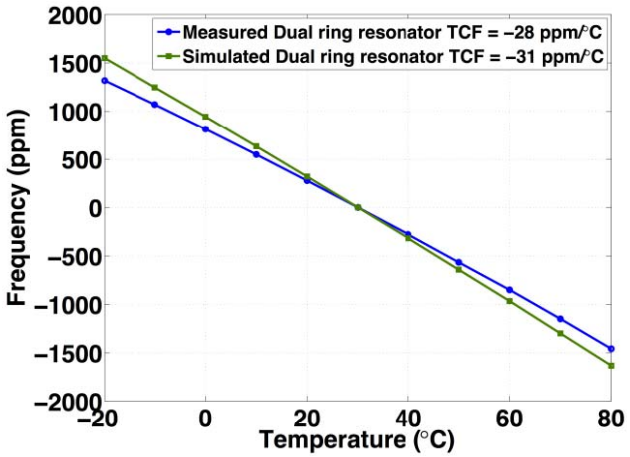

Fig. 7. Measured and simulated frequency of a dual ring resonator over temperature. Error bars are too small to show.

fully-anisotropic materials properties. We can account for the temperature dependence of 3 different orientations of this resonator, relying only on one separately-determined parameter – the pressure inside the encapsulation. We find that single set of materials properties and a single value for the pressure is sufficient to accurately predict the Q of all of these resonators at all of these temperatures.

B. Dual Ring Resonator

The dual ring resonators were initially expected not to have strong TED due to the greatly-reduced strain gradients arising in the breathe mode of the rings and the extensional mode of the coupling bars, as compared to the strains in DETFs. This design has been a focus of interest for our group because of its potential to have very high Q and to reach the Akhiezer limit [10]. Here, we present the first model predictions for Q of this device based on the full set of mechanical and thermal properties for these resonators, including the anisotropy of the elastic constants.

Figure 7 compares measured and simulated frequency of the dual ring resonator over temperature. The comparison is consistent with the result for the DETF. Measured TCF is smaller than that of the DETF by 1 ppm/°C.

The first result is that inclusion of the crystalline anisotropy in the TED model leads to a significant increase in the predicted strength of TED in these resonators. In this case, it becomes clear that the anisotropy of the crystal creates unexpected strains within the extensional mode of the rings, and this causes significant TED. Additionally, the slight mismatch between the extensional modes of the rings and bars leads to additional stresses that were not expected to appear in this device, and which also cause increased TED. Comparison of the values of Q at room temperature in Table VII shows that the measured Q is only slightly less than the prediction from the TED model. Akhiezer damping is weaker than TED, but may explain the difference between the measurements and the TED model. A measurement of $Q(P)$ for this device was only available for a dual ring resonator with unspecified orientation and doping and is plotted in Figure 8. We have no reason to believe pressure of the cavity is >100 Pa which would correspond to the measured Q ~150,000 at room temperature. As explained later, we do have a more complete set of $Q(P)$ measurements for the DRG from this same wafer, which lead to an estimate of P ~0.6Pa. In these experiments, it is clear that the $Q(P)$ does not contribute to the Q of the dual-ring resonator, and so we neglect this contribution.

TABLE VII
COMPARISON OF QUALITY FACTOR AT ROOM TEMPERATURE FOR THE DUAL RING RESONATOR. QMEAS FROM MEASUREMENT, QTED FROM FULLY COUPLED SIMULATION AND QAKE FROM THE AKHIEZER MODEL OF (2.2)

Q_{meas}	Q_{TED}	Q_{AKE}
147,000	153,000	3,900,000

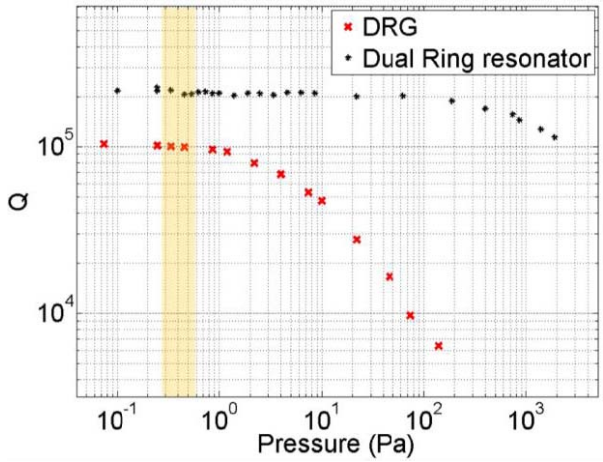

Fig. 8. Measured pressure dependence of quality factor of a representative dual ring resonator and a disk resonator from the same wafer.

Further, we neglect any contribution from anchor damping in this device, as we are able to fully account for the observed $Q(T)$ without invoking anchor damping. This result came as a surprise to us, as we had previously believed that the modest Q of these devices could not result from TED or AKE, and that anchor damping was the most logical candidate for the loss. However, by measuring the temperature dependence of the Q, it becomes clear that anchor damping cannot be a dominant source of loss in these devices, illustrating the great value in measuring Q over temperature.

We are able to calculate the temperature dependence of the AKE contribution to the Q, and construct a model for dissipation in this device that incorporates the AKE and TED contributions, without any adjusted parameters. Figures 9 and Figure 10 illustrate that the Q of the dual ring resonator is primarily TED limited. The overall modeled Q is given by $Q_{model}^{-1} = Q_{TED}^{-1} + Q_{AKE}^{-1}$. As can be seen, the modeled Q predicts all data points within the uncertainty of the material properties. The uncertainty in the modeled results is consistent over the temperature range, and reflects the uncertainty in the materials properties used as the basis for these model predictions. The larger error bars on the measured values at low temperature are due to temperature instability in the oven. For this data set, TED simulations with nominal material properties are exact for three data points in mid range temperature.

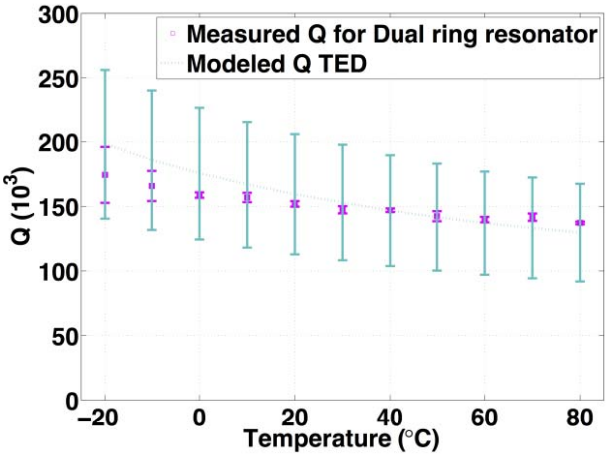

Fig. 9. Measured and simulated Q of the dual ring resonator. The dashed line goes through the values from fully coupled TED simulations with typical material properties of SCS and the large error bars correspond to simulated values with uncertainty in material properties as in Table V. The error bars on measured data points are from multiple measurements of Q at each temperature.

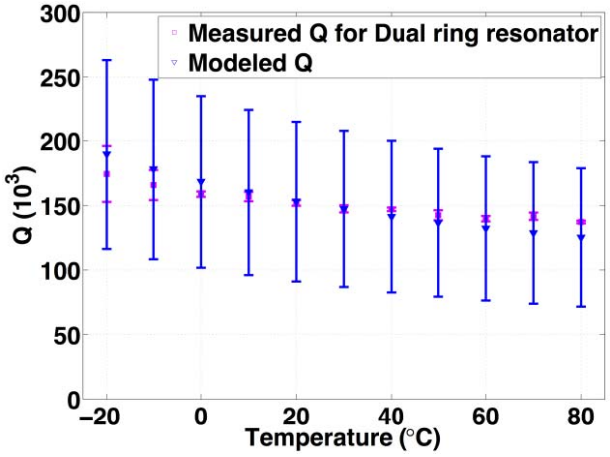

Fig. 10. Measured and overall modeled Q of the dual ring resonator. Modeled Q values represent $Q_{model}^{-1} = Q_{TED}^{-1} + Q_{AKE}^{-1}$. Larger error bars on the modeled values correspond to the uncertainty in the material properties in calculations of Q_{TED} and Q_{AKE}.

The uncertainty in material properties produces a confidence bound of 40% for the modeled values.

A close examination of the data and the models for this device show that there is not an exact agreement between model predictions and Q measurements across the temperature range – there is some discrepancy between the trends. However, it is important to appreciate that these models do not include any adjustable parameters, can be executed using modern simulation tools using published materials property data, and represent some of the first predictions of Q for a complex resonator which are able to account for the measurements without invoking additional, sometimes unspecified loss mechanisms.

C. Disk Resonator (DRG)

The disk resonator is based on an important and widely investigated gyroscope design proposed by Challoner [52]. The disk structure is useful for angular rate sensing because it

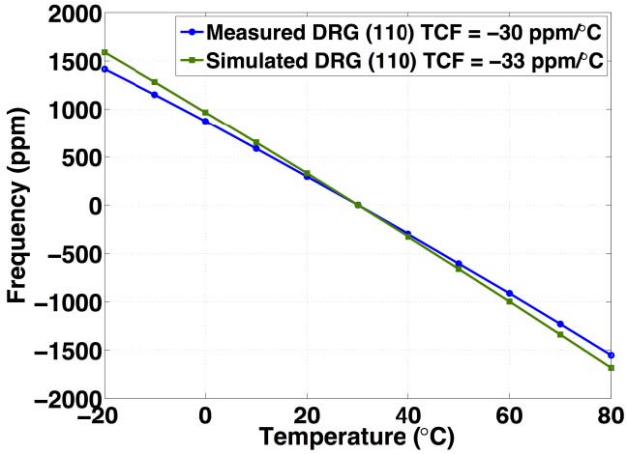

Fig. 11. Measured and simulated frequency of the disk resonator over temperature for the (110) wine glass mode that aligns with ⟨110⟩ crystal direction.

may be driven into either of a pair of *wine glass* modes with fixed relative angular displacement [53]–[55]. The design is compatible with the in-plane drive and sense geometry that is easily realized in our epi-seal process and the modes of this device are easily driven and sensed. Further, the cylindrical symmetry of this device about a central anchor suppresses anchor damping, especially if fabricated in a process that does not introduce misalignment between device and anchor, such as the epi-seal process used in this work. The TED in complex mode structures such as the DRG has never been accurately modeled, because of the presumed lack of capacity for handling such a complex structure on a desktop computer. Instead, designers have relied on empirical measurements on suites of designs to improve the performance of this device. Accurate models for the Q of these designs could lead to important performance improvements such as improved gyroscope resolution, or a path to smaller, less-expensive gyroscopes.

Due to the crystalline anisotropy of SCS, the frequencies of the two wine glass modes of the DRG align with the ⟨110⟩ crystal axis (to be called the (110) mode) and the ⟨100⟩ crystal (to be called the (100) mode.), and are generally separated by several percent in frequency. This "frequency split" can be tuned out by electrostatic tuning or mechanical design [63], but the relationship between design and quality factor has not been carefully examined. Because of the complex interplay between the movements of the rings, the stresses in the connecting bars, and the interaction between thermal and mechanical domains, there has been no successful "reduction to intuition" that would guide designers interested in the quality factor of the DRG.

As shown in Figure 11, measured and simulated frequency of the DRG (110) mode are consistent with the other two devices and measured and simulated TCFs are similar as expected for the same wafer doping. Recent results [64] show that TCF of the three devices varies significantly as a function of both doping level and type.

Table VIII compares the measured Q and the simulated TED contribution for the (110) mode at room temperature.

TABLE VIII
COMPARISON OF QUALITY FACTOR AT ROOM TEMPERATURE FOR THE DISK RESONATOR. QMEAS FROM MEASUREMENT, QTED FROM FULLY COUPLED SIMULATION AND QAKE FROM THE AKHIEZER MODEL OF (2.2)

Q_{meas}	Q_{TED}	$Q_{pressure}$	Q_{anchor}	Q_{AKE}
103,000	131,000	283,000	8,000,000	92,000,000

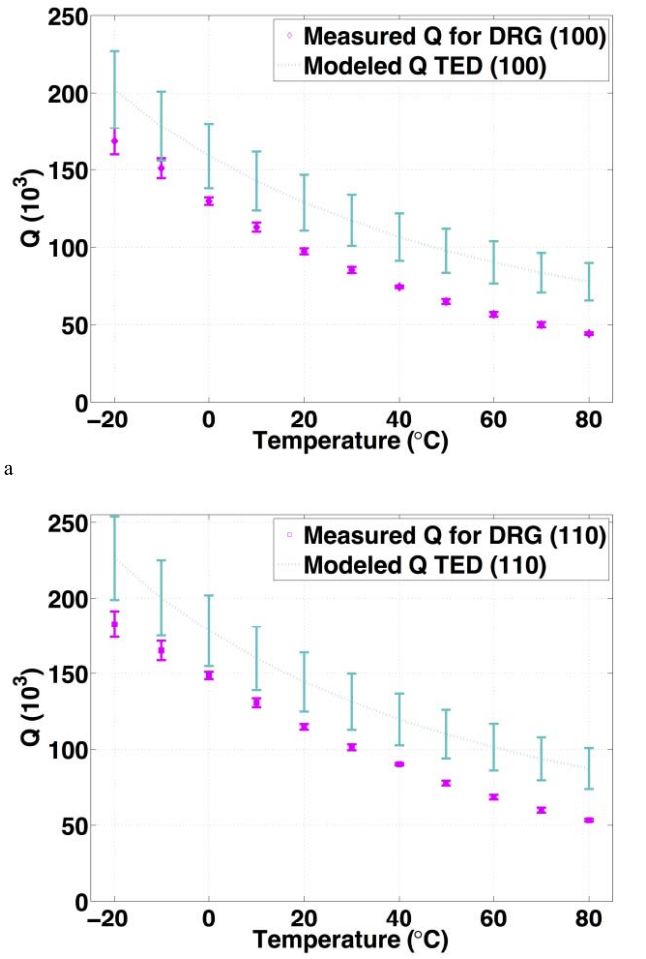

Fig. 12. Measured and simulated Q of the pair of wine glass mode of the disk resonator aligned with a) ⟨100⟩ direction, and b) ⟨110⟩ direction. The dashed line goes through the values from fully coupled TED simulations with typical material properties of SCS and the error bars correspond to simulated values with uncertainty in the material properties as in Table V. The error bars on measured data points are from multiple measurements of Q at each temperature.

Because Akhiezer damping is insignificant at the low frequency of this mode, the discrepancy between the predictions for the TED contribution and the measured result may arise from anchor damping or pressure damping.

In Figure 12, we compare the measured Q with the Q from TED simulations over temperature for the wine glass mode pair. For each TED simulation, we obtain two distinct Q values for the two modes as a result of silicon anisotropy. We find that Q compares well to TED predictions but measurements show a greater reduction in Q at higher temperatures than can be found in the TED simulation. We examine pressure damping as a possible candidate for additional dissipation because the

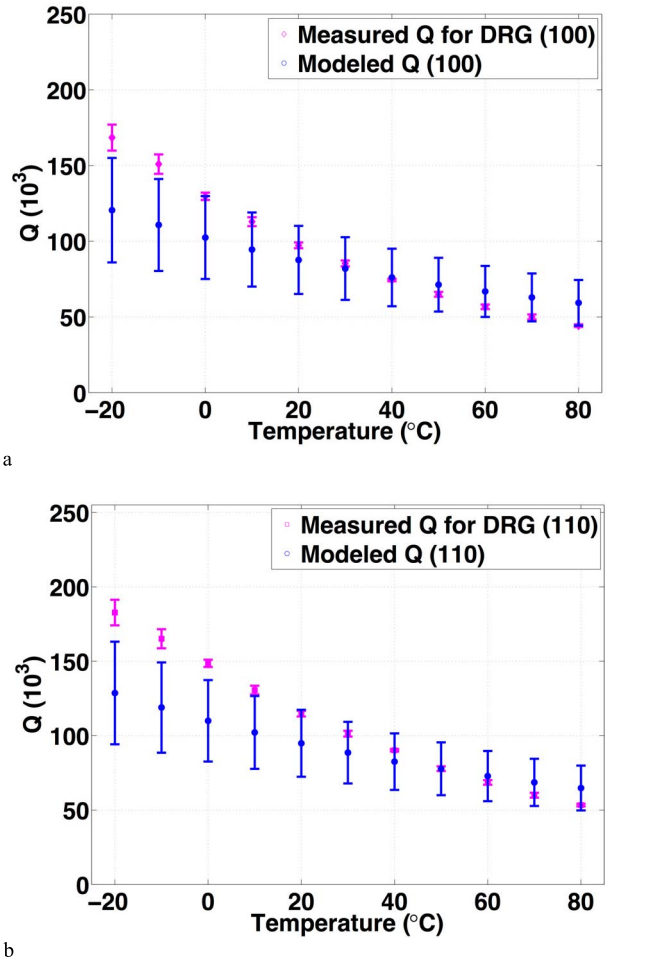

Fig. 13. Measured and overall modeled Q of the pair of wine glass mode of the disk resonator aligned with a) ⟨100⟩ direction, and b) ⟨110⟩ direction. Modeled Q values represent $Q_{model} = (Q_{TED}^{-1} + Q_{pressure}^{-1} + Q_{anchor}^{-1})^{-1}$. Models are obtained for equal pressure and anchor damping in both modes. Larger error bars on the modeled values correspond to the uncertainty in the material properties and pressure.

"signature" of pressure damping is for more damping at high temperatures.

Our model for the overall Q is obtained by representing it as the sum of contributions from TED, pressure and anchor damping $Q_{model}^{-1} = Q_{TED}^{-1} + Q_{pressure}^{-1} + Q_{anchor}^{-1}$. We assume that anchor damping is a temperature-independent contribution, and the pressure damping has the $T^{-1/2}$ dependence that is a signature of this term. We know from experiments on a FIB-vented resonator that the Q at vacuum is only slightly better than the Q in the package, with the pressure in the package for these devices determined to be between 0.3Pa and 0.6Pa. We use this experiment to determine the pressure damping at room temperature, and apply the $T^{-1/2}$ scaling to determine the complete temperature dependence of this term.

After calculating the temperature dependence of the pressure damping and fitting the residual to a temperature-independent anchor-damping term, the final plots of the model results and the experimental results are shown in Figure 13 for both mode orientations, as a function of temperature. We find that the Q of the DRG is mostly limited by TED with small corrections possible from pressure and anchor damping.

This important and surprising result shows that it should be possible to improve the Q of the DRG by as much as 10X by simulation-guided design modifications, and we are presently exploring this possibility.

V. Conclusions

We have shown that by accurately modeling the most relevant contributions to damping, very accurate quantitative predictions of the quality factor for complex MEMS resonators can be produced. We employ the fully coupled equations of thermoelasticity to compute Q from thermoelastic dissipation. Q of AKE is obtained analytically and the contributions of pressure and anchor damping are evaluated by fitting a scaling model to the experimental data with correct temperature scaling, combined with other independent determinations of these remaining terms. By implementing the fully anisotropic representation and temperature dependence of the relevant mechanical properties, we are able to predict quality factors of set of fundamentally different resonator designs. In all three cases of different kinds of resonator design, the resonators are shown to be primarily limited by TED. The crystallographic and temperature dependence of Q and f is mostly determined by the temperature dependence of the materials parameters, such as thermal conductivity and specific heat, which determine the strength of TED. Through this work, we hope to convince the reader that it is now possible to use the full anisotropic representation of the elastic constants of silicon, along with published data for the temperature dependence of other materials parameters, and build detailed, quantitative, predictive models of Q in MEMS resonators.

References

[1] C. Zener, "Internal friction in solids. I. Theory of internal friction in reeds," *Phys. Rev.*, vol. 52, p. 230, Aug. 1937.

[2] C. Zener, "Internal friction in solids II. General theory of thermoelastic internal friction," *Phys. Rev.*, vol. 53, p. 90, Jan. 1938.

[3] K. L. Ekinci and M. L. Roukes, "Nanoelectromechanical systems," *Rev. Sci. Instrum.*, vol. 76, no. 6, p. 061101, 2005.

[4] K. Y. Yasumura *et al.*, "Quality factors in micron- and submicron-thick cantilevers," *J. Microelectromech. Syst.*, vol. 9, no. 1, pp. 117–125, Mar. 2000.

[5] A. Duwel, R. N. Candler, T. W. Kenny, and M. Varghese, "Engineering MEMS resonators with low thermoelastic damping," *J. Microelectromech. Syst.*, vol. 15, no. 6, pp. 1437–1445, Dec. 2006.

[6] R. N. Candler *et al.*, "Impact of geometry on thermoelastic dissipation in micromechanical resonant beams," *J. Microelectromech. Syst.*, vol. 15, no. 4, pp. 927–934, Aug. 2006.

[7] T. V. Roszhart, "The effect of thermoelastic internal friction on the Q of micromachined silicon resonators," in *IEEE Solid-State Sens. Actuator Workshop, Tech. Dig.*, Jun. 1990, pp. 13–16.

[8] R. Lifshitz and M. L. Roukes, "Thermoelastic damping in micro- and nanomechanical systems," *Phys. Rev. B*, vol. 61, no. 8, p. 5600, 2000.

[9] J. Yang, T. Ono, and M. Esashi, "Energy dissipation in submicrometer thick single-crystal silicon cantilevers," *J. Microelectromech. Syst.*, vol. 11, no. 6, pp. 775–783, Dec. 2002.

[10] S. Ghaffari *et al.*, "Quantum limit of quality factor in silicon micro and nano mechanical resonators," *Sci. Rep.*, vol. 3, Nov. 2013, Art. ID 3244.

[11] A. E. Duwel, J. Lozow, C. J. Fisher, T. Phillips, R. H. Olsson, and M. Weinberg, "Thermal energy loss mechanisms in micro- to nanoscale devices," *Proc. SPIE, Micro- Nanotechnol. Sensors, Syst., Appl. III*, vol. 8031, pp. 80311C-1–80311C-14, May 2011.

[12] R. Tabrizian, M. Rais-Zadeh, and F. Ayazi, "Effect of phonon interactions on limiting the f.Q product of micromechanical resonators," in *Proc. IEEE TRANSDUCERS*, Jun. 2009, pp. 2131–2134.

[13] S. A. Chandorkar, M. Agarwal, R. Melamud, R. N. Candler, K. E. Goodson, and T. W. Kenny, "Limits of quality factor in bulk-mode micromechanical resonators," in *Proc. IEEE 21st Int. Conf. MEMS*, Jan. 2008, pp. 74–77.

[14] V. T. Srikar and S. D. Senturia, "Thermoelastic damping in fine-grained polysilicon flexural beam resonators," *J. Microelectromech. Syst.*, vol. 11, no. 5, pp. 499–504, Oct. 2002.

[15] R. Abdolvand, "Thermoelastic damping in trench-refilled polysilicon resonators," in *Proc. 12th Int. Conf. TRANSDUCERS, Solid-State Sens., Actuators, Microsyst.*, Jun. 2003, pp. 324–327.

[16] S. Prabhakar and S. Vengallatore, "Theory of thermoelastic damping in micromechanical resonators with two-dimensional heat conduction," *J. Microelectromech. Syst.*, vol. 17, no. 2, pp. 494–502, Apr. 2008.

[17] S. Prabhakar and S. Vengallatore, "Thermoelastic damping in hollow and slotted microresonators," *J. Microelectromech. Syst.*, vol. 18, no. 3, pp. 725–735, Jun. 2009.

[18] P. Mohanty, D. A. Harrington, K. L. Ekinci, Y. T. Yang, M. J. Murphy, and M. L. Roukes, "Intrinsic dissipation in high-frequency micromechanical resonators," *Phys. Rev. B*, vol. 66, p. 085416, Aug. 2002.

[19] S. Reid *et al.*, "Mechanical dissipation in silicon flexures," *Phys. Lett. A*, vol. 351, nos. 4–5, pp. 205–211, 2006.

[20] A. H. Nayfeh and M. I. Younis, "Modeling and simulations of thermoelastic damping in microplates," *J. Micromech. Microeng.*, vol. 14, no. 12, pp. 1711–1717, 2004.

[21] S. J. Wong, C. H. J. Fox, and S. McWilliam, "Thermoelastic damping of the in-plane vibration of thin silicon rings," *J. Sound Vibrat.*, vol. 293, nos. 1–2, pp. 266–285, 2006.

[22] P. Li, Y. Fang, and R. Hu, "Thermoelastic damping in rectangular and circular microplate resonators," *J. Sound Vibrat.*, vol. 331, no. 3, pp. 721–733, 2012.

[23] S. Evoy, A. Olkhovets, L. Sekaric, J. M. Parpia, H. G. Craighead, and D. W. Carr, "Temperature-dependent internal friction in silicon nanoelectromechanical systems," *Appl. Phys. Lett.*, vol. 77, no. 15, p. 2397, 2000.

[24] B. Kim *et al.*, "Temperature dependence of quality factor in MEMS resonators," *J. Microelectromech. Syst.*, vol. 17, no. 3, pp. 755–766, Jun. 2008.

[25] B. H. Houston, D. M. Photiadis, M. H. Marcus, J. A. Bucaro, X. Liu, and J. F. Vignola, "Thermoelastic loss in microscale oscillators," *Appl. Phys. Lett.*, vol. 80, no. 7, pp. 1300–1302, 2001.

[26] J. Yang, T. Ono, and M. Esashi, "Surface effects and high quality factors in ultrathin single-crystal silicon cantilevers," *Appl. Phys. Lett.*, vol. 77, no. 23, pp. 3860–3862, 2000.

[27] X. Liu *et al.*, "On the modes and loss mechanisms of a high Q mechanical oscillator," *Appl. Phys. Lett.*, vol. 78, no. 10, pp. 1346–1348, 2001.

[28] F. R. Blom, S. Bouwstra, M. Elwenspoek, and J. H. J. Fluitman, "Dependence of the quality factor of micromachined silicon beam resonators on pressure and geometry," *J. Vac. Sci. Technol. B*, vol. 10, no. 1, pp. 19–26, 1992.

[29] Y. Sun, D. Fang, and A. K. Soh, "Thermoelastic damping in microbeam resonators," *Int. J. Solids Struct.*, vol. 43, no. 10, pp. 3213–3229, May 2006.

[30] C. Tu and J. E.-Y. Lee, "Crystallographic effects on energy dissipation in high-Q silicon bulk-mode resonators," *J. Microelectromech. Syst.*, vol. 22, no. 2, pp. 262–264, Apr. 2013.

[31] R. Ardito, C. Comi, A. Corigliano, and A. Frangi, "Solid damping in micro electro mechanical systems," *Meccanica*, vol. 43, no. 4, pp. 419–428, 2008.

[32] X. Guo, Y.-B. Yi, and S. Pourkamali, "A finite element analysis of thermoelastic damping in vented MEMS beam resonators," *Int. J. Mech. Sci.*, vol. 74, pp. 73–82, Sep. 2013.

[33] B. Le Foulgoc *et al.*, "Highly decoupled single-crystal silicon resonators: An approach for the intrinsic quality factor," *J. Micromech. Microeng.*, vol. 16, no. 6, pp. S45–S53, 2006.

[34] I. Mizushima, T. Sato, S. Taniguchi, and Y. Tsunashima, "Empty-space-in-silicon technique for fabricating a silicon-on-nothing structure," *Appl. Phys. Lett.*, vol. 77, no. 20, pp. 3290–3292, Nov. 2000.

[35] R. N. Candler *et al.*, "Single wafer encapsulation of MEMS devices," *IEEE Trans. Adv. Packag.*, vol. 26, no. 3, pp. 227–232, Aug. 2003.

[36] D. R. Sherman, "An investigation of MEMS anchor design for optimal stiffness and damping," M.S. thesis, Dept. Mech. Eng., Univ. California, Berkeley, CA, USA, 1996.

[37] Z. Hao, A. Erbil, and F. Ayazi, "An analytical model for support loss in micromachined beam resonators with in-plane flexural vibrations," *Sens. Actuators A, Phys.*, vol. 109, nos. 1–2, pp. 156–164, Dec. 2003.

[38] D. M. Photiadis and J. A. Judge, "Attachment losses of high Q oscillators," *Appl. Phys. Lett.*, vol. 85, no. 3, pp. 482–484, Jul. 2004.

[39] Y.-H. Park and K. C. Park, "High-fidelity modeling of MEMS resonators. Part I. Anchor loss mechanisms through substrate," *J. Microelectromech. Syst.*, vol. 13, no. 2, pp. 238–247, Apr. 2004.

[40] D. S. Binder, E. Quevy, T. Koyama, S. Govindjee, J. W. Demmel, and R. T. Howe, "Anchor loss simulation in resonators," in *Proc. 18th IEEE Int. Conf. MEMS*, Jan./Feb. 2005, pp. 133–136.

[41] J. E.-Y. Lee, J. Yan, and A. A. Seshia, "Study of lateral mode SOI-MEMS resonators for reduced anchor loss," *J. Micromech. Microeng.*, vol. 21, no. 4, p. 045010, 2011.

[42] A. Frangi, M. Cremonesi, A. Jaakkola, and T. Pensala, "Analysis of anchor and interface losses in piezoelectric MEMS resonators," *Sens. Actuators A, Phys.*, vol. 190, no. 1, pp. 127–135, Feb. 2013.

[43] A. Akhieser, "On the absorption of sound in solids," *J. Phys. Akad. Nauk-Leningrad*, vol. 1, pp. 277–287, 1939.

[44] H. J. Maris, "Interaction of sound waves with thermal phonons in dielectric crystals," *Phys. Acoust.*, vol. 8, pp. 279–345, 1971.

[45] W. Nowacki, *Thermoelasticity*. New York, NY, USA: Pergamon, 1962.

[46] COMSOL. (2013). *COMSOL Multiphysics Software, V. 4.3a*. [Online]. Available: http://www.comsol.com

[47] C. Tu and J. E.-Y. Lee, "Increased dissipation from distributed etch holes in a lateral breathing mode silicon micromechanical resonator," *Appl. Phys. Lett.*, vol. 101, no. 2, p. 023504, 2012.

[48] M. A. Hopcroft, W. D. Nix, and T. W. Kenny, "What is the Young's modulus of silicon?" *J. Microelectromech. Syst.*, vol. 19, no. 2, pp. 229–238, Apr. 2010.

[49] H. K. Lee, B. Kim, R. Melamud, M. A. Hopcroft, J. C. Salvia, and T. W. Kenny, "Influence of the temperature dependent nonlinearities on the performance of micromechanical resonators," *Appl. Phys. Lett.*, vol. 99, no. 19, p. 194102, 2011.

[50] M. A. Hopcroft *et al.*, "Using the temperature dependence of resonator quality factor as a thermometer," *Appl. Phys. Lett.*, vol. 91, no. 1, p. 013505, 2007.

[51] E. J. Ng, H.-K. Lee, C.-H. Ahn, R. Melamud, and T. W. Kenny, "Stability of silicon microelectromechanical systems resonant thermometers," *IEEE Sensors J.*, vol. 13, no. 3, pp. 987–993, Mar. 2013.

[52] K. V. Shcheglov and A. D. Challoner, "Isolated planar gyroscope with internal radial sensing and actuation," U.S. Patent 7 040 163, May 9, 2006.

[53] M. W. Putty, "A micromachined vibrating ring gyroscope," Ph.D. dissertation, Dept. Elect. Eng. Comput. Sci., Univ. Michigan, Ann Arbor, MI, USA, 1995.

[54] F. Ayazi and K. Najafi, "A HARPSS polysilicon vibrating ring gyroscope," *J. Microelectromech. Syst.*, vol. 10, no. 2, pp. 169–179, Jun. 2001.

[55] S. Ghaffari, C. H. Ahn, E. J. Ng, S. Wang, and T. W. Kenny, "Crystallographic effects in modeling fundamental behavior of MEMS silicon resonators," *Microelectron. J.*, vol. 44, no. 7, pp. 586–591, 2013.

[56] N. Mehanathan, V. Tavassoli, P. Shao, L. Sorenson, and F. Ayazi, "Invar-36 micro hemispherical shell resonators," in *Proc. IEEE 27th Int. Conf. MEMS*, Jan. 2014, pp. 40–43.

[57] Z. Wu *et al.*, "Piezoelectrically transduced high-Q silica micro resonators," in *Proc. IEEE 26th Int. Conf. MEMS*, Taipei, Taiwan, Jan. 2013, pp. 122–125.

[58] S. Ghaffari Jahromi, "Comprehensive modeling of complex silicon microelectromechanical (MEMS) resonators," Ph.D. dissertation, Dept. Mech. Eng., Stanford Univ., Stanford, CA, USA, 2014.

[59] S. Prabhakar, M. P. Païdoussis, and S. Vengallatore, "Analysis of frequency shifts due to thermoelastic coupling in flexural-mode micromechanical and nanomechanical resonators," *J. Sound Vibrat.*, vol. 323, nos. 1–2, pp. 385–396, 2009.

[60] A. K. Samarao and F. Ayazi, "Temperature compensation of silicon resonators via degenerate doping," *IEEE Trans. Electron Devices*, vol. 59, no. 1, pp. 87–93, Jan. 2012.

[61] J. J. Hall, "Electronic effects in the elastic constants of n-type silicon," *Phys. Rev.*, vol. 161, no. 3, pp. 756–761, 1967.

[62] M. Shahmohammadi, B. P. Harrington, and R. Abdolvand, "Turnover temperature point in extensional-mode highly doped silicon microresonators," *IEEE Trans. Electron Devices*, vol. 60, no. 3, pp. 1213–1220, Mar. 2013.

[63] C. H. Ahn *et al.*, "Geometric compensation of (100) single crystal silicon disk resonating gyroscope for mode-matching," in *Proc. IEEE Int. Conf. Transducers Eurosensors XXVII*, Jun. 2013, pp. 1723–1726.

[64] E. J. Ng *et al.*, "Localized, degenerately doped epitaxial silicon for temperature compensation of resonant MEMS systems," in *Proc. IEEE Int. Conf. Transducers Eurosensors XXVII*, Jun. 2013, pp. 2419–2422.

[65] E. J. Ng, V. A. Hong, Y. Yang, C. H. Ahn, C. L. M. Everhart, and T. W. Kenny, "Temperature dependence of the elastic constants of doped silicon," *J. Microelectromech. Syst.*, to be published.

[66] C. Bourgeois, E. Steinsland, N. Blanc, and N. F. de Rooij, "Design of resonators for the determination of the temperature coefficients of elastic constants of monocrystalline silicon," in *Proc. IEEE Int. Freq. Control Symp.*, 1997, pp. 791–799.

[67] P. Flubacher, A. J. Leadbetter, and J. A. Morrison, "The heat capacity of pure silicon and germanium and properties of their vibrational frequency spectra," *Philosoph. Mag.*, vol. 4, no. 39, pp. 273–294, 1959.

[68] Y. Okada and Y. Tokumaru, "Precise determination of lattice parameter and thermal expansion coefficient of silicon between 300 and 1500 K," *J. Appl. Phys.*, vol. 56, no. 2, pp. 314–320, Jul. 1984.

[69] W. Liu, K. Etessam-Yazdani, R. Hussin, and M. Asheghi, "Modeling and data for thermal conductivity of ultrathin single-crystal SOI layers at high temperature," *IEEE Trans. Electron Devices*, vol. 53, no. 8, pp. 1868–1876, Aug. 2006.

[70] M. A. Hopcroft, "Temperature-stabilized silicon resonators for frequency," Ph.D. dissertation, Dept. Mech. Eng., Stanford Univ., Stanford, CA, USA, 2007.

Shirin Ghaffari received the B.S. degree in aerospace engineering from the Sharif University of Technology, Tehran, Iran, in 2007, and the M.S. and Ph.D. degrees from Stanford University, Stanford, CA, USA, in 2009 and 2014, respectively. She is currently with Apple Inc., Cupertino, CA, USA.

Eldwin Jiaqiang Ng received the B.S. degree in mechanical engineering from the University of California at Berkeley, Berkeley, CA, USA, in 2009, and the M.S. degree in mechanical engineering from Stanford University, Stanford, CA, USA, in 2012, where he is currently pursuing the Ph.D. degree with the Department of Mechanical Engineering under a scholarship from the Agency for Science, Technology, and Research, Singapore. His research interests include microfabrication technologies, RF resonators, and MEMS sensors and switches.

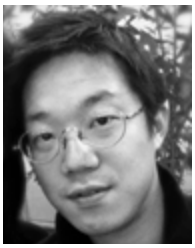

Chae Hyuck Ahn received the B.S. degree in mechanical engineering from Seoul National University, Seoul, Korea, in 2010, and the M.S. degree in mechanical engineering from Stanford University, Stanford, CA, USA, in 2012, where he is currently pursuing the Ph.D. degree with the Department of Mechanical Engineering under a Kwanjeong Scholarship. His research interests include resonant thermometers, micromachined disk resonating gyroscopes, silicon anisotropy compensation by geometric design, and the integration of inertial measurement units and timing references.

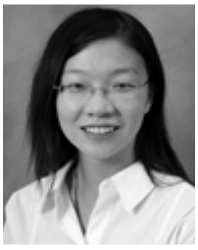

Yushi Yang received the dual Bachelor's degree in mechanical engineering from Purdue University, West Lafayette, IN, USA, and Shanghai Jiao Tong University, Shanghai, China, in 2011, and the M.S. degree in mechanical engineering from Stanford University, Stanford, CA, USA, in 2013, where she is currently pursuing the Ph.D. degree with the Department of Mechanical Engineering. Her research interests include studying the nonlinear behavior of bulk-mode MEMS resonators, and analyzing the phase noise performance of MEMS oscillators under large driving conditions.

Shasha Wang received the B.S. degree from the Department of Microelectronics, Peking University, Beijing, China, in 2006, and the M.S. and Ph.D. degrees in electrical engineering from Stanford University, Stanford, CA, USA, in 2008 and 2013, respectively. From 2012 to 2013, she was with Fairchild Semiconductor, San Jose, CA, as a MEMS Design Engineer working on six-axis accelerometer, and gyroscope design and characterization. She is currently with Apple Inc., Cupertino, CA, as a Sensing Hardware Integration Engineer.

Vu A. Hong received the B.S. degree in mechanical engineering from the Massachusetts Institute of Technology, Cambridge, MA, USA, in 2010, and the M.S. degree in mechanical engineering from Stanford University, Stanford, CA, USA, in 2012, where he is currently pursuing the Ph.D. degree with the Department of Mechanical Engineering.

Mr. Hong was the recipient of the National Science Foundation Graduate Research Fellowship.

Thomas W. Kenny received the B.S. degree in physics from the University of Minnesota, Minneapolis, MN, USA, in 1983, and the M.S. and Ph.D. degrees in physics from the University of California at Berkeley, Berkeley, CA, USA, in 1987 and 1989, respectively. From 1989 to 1993, he was with the Jet Propulsion Laboratory, National Aeronautics and Space Administration, Pasadena, CA, where his research focused on the development of electron-tunneling high-resolution microsensors. In 1994, he joined the Department of Mechanical Engineering, Stanford University, Stanford, CA, where he directs microsensor-based research in a variety of areas, including resonators, wafer-scale packaging, cantilever beam force sensors, microfluidics, and novel fabrication techniques for micromechanical structures. He is the Founder and CTO of Cooligy Inc. (now a division of Emerson), Mountain View, CA, a microfluidics chip cooling component manufacturer, and the Founder and a Board Member of SiTime Corporation, Sunnyvale, CA, a developer of timing references using MEMS resonators. He is currently a Bosch Faculty Development Scholar and was the General Chairman of the 2006 Hilton Head Solid State Sensor, Actuator, and Microsystems Workshop, and will be the General Chair of the upcoming Transducers 2015 meeting in Anchorage, AK, USA. From 2006 to 2010, he was on leave to serve as the Program Manager of the Microsystems Technology Office at the Defense Advanced Research Projects Agency, Arlington, VA, USA, starting and managing programs in thermal management, nanomanufacturing, and manipulation of Casimir forces, and received the Young Faculty Award. He has authored or co-authored over 250 scientific papers and holds 50 issued patents.